# Multicomponent AM–FM Demodulation via Periodicity-Based Algebraic Separation and Energy-Based Demodulation

Balasubramaniam Santhanam, *Member, IEEE*, and Petros Maragos, *Fellow, IEEE*

***Abstract*—Previously investigated multicomponent AM–FM demodulation techniques either assume that the individual component signals are spectrally isolated from each other or that the components can be isolated by linear time-invariant filtering techniques and, consequently, break down in the case where the components overlap spectrally or when one of the components is stronger than the other. In this paper, we present a nonlinear algorithm for the separation and demodulation of discrete-time multicomponent AM–FM signals. Our approach divides the demodulation problem into two independent tasks: algebraic separation of the components based on periodicity assumptions and then monocomponent demodulation of each component by instantaneously tracking and separating its source energy into its amplitude and frequency parts. The proposed new algorithm avoids the shortcomings of previous approaches and works well for extremely small spectral separations of the components and for a wide range of relative amplitude/power ratios. We present its theoretical analysis and experimental results and outline its application to demodulation of cochannel FM voice signals.**

***Index Terms*—Algebraic separation, cochannel and adjacent-channel signal separation problem, demodulation, energy operators, multicomponent AM–FM signals, periodicity.**

## I. INTRODUCTION

MONOCOMPONENT AM–FM signals are sine waves $s(t) = a(t)\cos[\phi(t)]$ whose amplitude $a(t)$ and instantaneous frequency $\omega(t) = d\phi(t)/dt$ are time-varying quantities. Amplitude modulation (AM) and/or frequency modulation (FM) find extensive use in human-made communication systems [40] and are often present in signals created and processed by biological systems. For purposes of data processing by digital computers, in this paper we focus on *discrete-time*[1] AM–FM signals modeled (over finite time intervals) as

$$s[n] = A[n]\cos(\phi[n]) = A[n]\cos\left(\int_0^n \Omega[k]dk + \theta\right)$$
$$\Omega[n] \equiv \frac{d\phi}{dn}[n]$$

where $A[n]$ and $\Omega[n]$ are the instantaneous amplitude (IA) and angular frequency (IF) information signals.

*Multicomponent* AM–FM signals are superpositions of monocomponent AM–FM signals

$$x[n] \equiv \sum_{i=1}^{M} A_i[n]\cos\underbrace{\left(\int_0^n \Omega_i[k]dk + \theta_i\right)}_{\phi_i[n]}, \qquad M \geq 2 \quad (1)$$

where $\{A_i[n], \Omega_i[n]\}$ are the IF and IA information signals corresponding to the $i$th component. Each component IF signal is of the general form $\Omega_i[n] = \Omega_{ci} + \Omega_{mi}q_i[n]$, where $\Omega_{ci}$ is the carrier frequency of the $i$th component, $\Omega_{mi}$ is its maximum frequency deviation, and $q_i[n]$ is its normalized information signal with $|q_i[n]| \leq 1$. For each AM–FM component $x_i[n]$, we assume that its instantaneous amplitude $A_i[n]$ and frequency $\Omega_i[n]$ do not vary too fast or too greatly compared with its carrier frequency $\Omega_{ci}$. Further, as explained in [1] and [2], for the decomposition of the composite signal $x[n]$ into its AM–FM components to be well defined, it is assumed that the instantaneous bandwidth, i.e., the instantaneous frequency spread of each component is narrow with respect to the instantaneous bandwidth of the composite signal. However, this assumption does not apply when the components overlap spectrally as in the cochannel and adjacent channel problems encountered in communication systems [36]. Thus, when there is a significant spectral overlap of the components, we shall assume that we know the number of components and hence their separation will incur some error due only to the overlap but not due to lack of information as to how many components exist.

[1]In the definition of discrete-time IF, for the differentiation $\Omega[n] = d\phi[n]/dn$ and the integration $\phi[n] = \int_0^n \Omega[k]dk + \theta$ we view the phase signal $\phi[n]$ and IF signal $\Omega[n]$ as functions of a continuous variable $n$, even if $n$ is a discrete time index. This assumes that both $\Omega[n]$ and $\phi[n]$ can be represented in terms of known mathematical functions that can be integrated or differentiated yielding known computable functions. This is not a restrictive assumption, since any real-valued discrete-time signal $\Omega[n]$ defined over a finite time interval can be represented via the DFT as a finite linear combination of cosines [7]. The discrete-time framework will also be needed by the matrix algebraic method for separating periodic components, as explained later.

Paper approved by B. L. Hughes, the Editor for Theory and Systems of the IEEE Communications Society. Manuscript received September 21, 1998; revised August 30, 1999. This work was supported by the U.S. National Science Foundation under Grant MIP-93963091 and Grant MIP-9421677. This paper was presented in part at the International Conference on Acoustics, Speech and Signal Processing, Munich, Germany, April 1997.

B. Santhanam was with the School of Electrical and Computer Engineering, Georgia Institute of Technology, Atlanta, GA 30332 USA. He is now with the Department of Electrical and Computer Engineering, University of New Mexico, Albuquerque, NM 87131-1356 USA (e-mail: bsanthan@eece.unm.edu).

P. Maragos was with the School of Electrical and Computer Engineering, Georgia Institute of Technology, Atlanta, GA 30332 USA. He is now with the Department of Electrical and Computer Engineering, National Technical University of Athens, 15773 Zografou, Athens, Greece (e-mail: maragos@cs.ntua.gr).

Publisher Item Identifier S 0090-6778(00)02277-7.

Multicomponent AM–FM signals form the basis for the general modeling of nonstationary signals as superpositions of modulated sinusoids, where each component occupies a narrow spectral band around its carrier frequency. In particular they find applications: a) for modeling cochannel and adjacent-channel interferences over communication channels, where one of the components models the desired signal and the other models the dominant interference [36]; b) in speech processing where speech signals are modeled as a superposition of time-varying acoustic resonances and each AM–FM component of the signal models a single resonance [7], [13]; c) for modeling clutter in high frequency radar [28] and in multiple target tracking applications [35]; and d) in the extraction of image textures via multicomponent two-dimensional spatial AM–FM signals [4], [9], [18].

The basic problem in processing AM–FM signals is *demodulation*, i.e., estimation of the information stored in the IA and IF signals given the composite signal. For monocomponent AM–FM signals many successful demodulation approaches exist, ranging from standard methods such as Hilbert transform demodulation [38] or phase-locked loops (PLL's) [25]–[27] to the recent *energy separation algorithm* (ESA) that tracks and demodulates the energy of the source producing the AM–FM signal using instantaneous nonlinear differential operators [6], [7]. While each of these monocomponent algorithms may have its advantages and disadvantages, they more or less offer a solution to the monocomponent AM–FM demodulation problem. For multicomponent AM–FM signals, however, there is the additional task of separating the components. Of course, when the components have approximately disjoint spectra this problem can be solved successfully via bandpass filtering and monocomponent demodulation. The challenging case, however, is when the components overlap spectrally and are no longer disjoint, as in the case of the cochannel problem [36].

Existing multicomponent AM–FM demodulation approaches include the following classes of algorithms.

1) State space estimation:
   a) cross-coupled digital phase-locked loop (CC-DPLL) algorithms [19], [24], [37];
   b) extended Kalman filtering (EKF) [16], [17], [20].
2) Techniques based on Hankel and Toeplitz matrices:
   a) the Hankel rank reduction (HRR) algorithm [32];
   b) the instantaneous Toeplitz determinant (ITD) algorithm [34].
3) Linear prediction:
   a) adaptive linear prediction using the exponentially-weighted RLS algorithm [29];
   b) the normalized LMS algorithm [30].
4) Energy demodulation:
   a) multiband-ESA (MESA) [5] that consists of bandpass filtering followed by monocomponent energy separation;
   b) the energy demodulation of mixtures (EDM) algorithm [11] that uses instantaneous nonlinear operators measuring cross-energies between components.
5) Maximum-likelihood estimation [33] that uses the discrete-time polynomial phase transform to initialize an iterative approach based on Newton's algorithm.

In contrast to the monocomponent case, all the above multicomponent AM–FM demodulation algorithms are still far from a general solution, work only in restricted ranges of spectral separation between components or relative amplitude/power ratios, and cannot deal with cross-over of the frequency tracks. In this paper, we present a solution to the general multicomponent AM–FM demodulation problem that greatly improves the above situation. Our approach divides the problem into two independent tasks of separation of components and then monocomponent demodulation of each component. For solving the separation task we extended an algebraic technique proposed in [12] and [15] for the separation of spectrally overlapping periodic signals. Specifically, we extended this algebraic separation technique to multicomponent AM–FM signals with periodic IF and IA information signals. For the monocomponent demodulation part, we use the energy-based method of ESA [7] due to its efficiency, low complexity and excellent time resolution. This combined new approach called the *periodic algebraic separation energy demodulation* (PASED) algorithm does not have the shortcomings of the other techniques and can deal with extremely small spectral separations and a wide range of amplitude/power ratios.

The contributions of this paper include: development of the two-component PASED algorithm for separating and demodulating two-component AM–FM signals; development of the multicomponent PASED algorithm, i.e., the generalization of the two-component algorithm to $M > 2$ components; comparison of the PASED algorithm with other existing demodulation algorithms; and preliminary application of PASED algorithm to the cochannel and adjacent-channel FM voice demodulation problem. Finally, we provide in the Appendix theoretical proofs of some results on the rank of the $M$-component separation matrix.

## II. PASED Algorithm

The PASED algorithm, whose block diagram is shown in Fig. 1, can be divided into two tasks: separation of the two-component AM–FM signal into components using periodicity—based signal modeling and algebraic separation techniques described in [12] and [15], and demodulation of the separated components into IF and IA information signals for each component using the *energy separation algorithm* (ESA) [6], [7].

### *A. Periodicity-Based Modeling and Algebraic Separation of the Components*

The *matrix algebraic separation* (MAS) algorithm for the separation of periodic signals that overlap both in the time- and frequency-domain has been investigated in [12] and [15]. The MAS algorithm distinguishes the components based on a slight difference in their periodicity. Consider a two-component periodic signal

$$x[n] = x_1[n] + x_2[n] = x_1[n + N_1] + x_2[n + N_2] \quad (2)$$

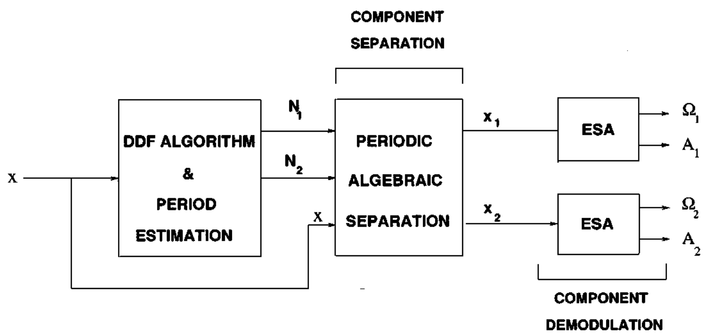


Fig. 1. Block diagram of the PASED algorithm.

where the fundamental periods of the components $x_1[n]$ and $x_2[n]$ are $N_1$ and $N_2$, respectively. Relating $N$ samples of the composite signal $x[n]$ to the samples of one fundamental period of the components yields the following system of linear equations, hereafter referred to as the *basic separation system*:

$$\underbrace{\begin{pmatrix} x[0] \\ x[1] \\ \vdots \\ x[N-1] \end{pmatrix}}_{\boldsymbol{x}} = \underbrace{\begin{pmatrix} \boldsymbol{I}_{N_1} & \boldsymbol{I}_{N_2} \\ \boldsymbol{I}_{N_1} & \boldsymbol{I}_{N_2} \\ \vdots & \vdots \end{pmatrix}}_{\boldsymbol{S}} \underbrace{\begin{pmatrix} x_1[0] \\ \vdots \\ x_1[N_1-1] \\ x_2[0] \\ \vdots \\ x_2[N_2-1] \end{pmatrix}}_{\boldsymbol{z}} \tag{3}$$

where $\boldsymbol{I}_{N_1}$ denotes the identity matrix of order $N_1$. The rank of the two-component separation matrix $\boldsymbol{S}$ is $r(\boldsymbol{S}) = N_1 + N_2 - \gcd(N_1, N_2)$ [12], [15]. Consequently, the basic separation system requires at least $N_1 + N_2 - 1$ composite signal samples to separate the components.

In the absence of noise, least-squares filtering is not required and increasing the number of composite signal samples used in the basic separation system over this minimum does not help as shown in Fig. 2. In the presence of noise however, least-squares smoothing is necessary and increasing the number of composite signal samples used in the basic separation system decreases the separation error as shown in Fig. 2.

The rank of the basic separation system for coprime component periods implies that one extra condition or equation is required to complete the system.[2] This is typically a dc value condition of the form

$$\sum_{n=0}^{N_1-1} x_1[n] = 0. \tag{4}$$

The dc value constraint corresponds to the assumption that the signal components are narrowband. This is a valid assumption to make, since the multicomponent AM–FM signal is modeled as a superposition of narrow-band bandpass components. The solution to the separation problem when the component periods are not coprime involves solving the separation system in partial subgroups. Suppose that $\gcd(N_1, N_2) = R$, so that

[2]The solution to the system $\boldsymbol{S}z = \boldsymbol{x}$ when the components periods are coprime is not unique in the sense that if $\{x_1[n], x_2[n]\}$ is a solution to the system, then $\{x_1[n] + c, x_2[n] - c\}$ is also a solution as noted in [12] and [15].

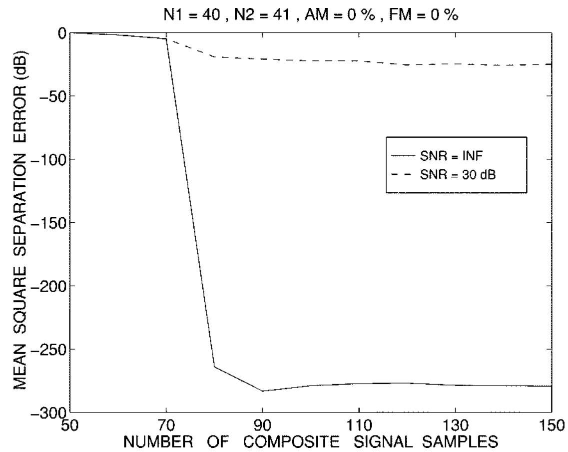


Fig. 2. Effect of AWGN on component separation in the PASED algorithm.

if $N_1 = RN_1'$ and $N_2 = RN_2'$, then $N_1'$ and $N_2'$ are mutually prime. The data is taken in subgroups by downsampling the components by a factor of $R$. Since the smaller periods are coprime, the separation problem is then solved for each subgroup. The union of the solutions from each group gives the total solution to the separation problem [12], [15]. The $R$ additional constraints/equations needed to complete the basic separation system are obtained as zero dc constraints on the subsampled components

$$\sum_{n=0}^{(N_1/R)-1} x_1[Rn+p] = 0, \qquad p = 0, 1, \cdots, R-1. \tag{5}$$

The solution to the component separation problem is then reformulated as the least-squares solution to the augmented linear system, hereafter referred to as the *augmented separation system*

$$\underbrace{\begin{pmatrix} \boldsymbol{S} \\ \boldsymbol{C} \end{pmatrix}}_{\tilde{\boldsymbol{S}}} z = \underbrace{\begin{pmatrix} \boldsymbol{x} \\ \mathbf{o} \end{pmatrix}}_{\tilde{\boldsymbol{x}}} \tag{6}$$

where the homogeneous dc value constraints at the scale of $R$ form the constraint matrix $\boldsymbol{C}$. The solution to this problem is equivalent to minimizing the quadratic form

$$\min_{\boldsymbol{z}} ||\boldsymbol{Sz} - \boldsymbol{x}||^2 + ||\boldsymbol{Cz}||^2.$$

The solution to this problem is of the form

$$\hat{\boldsymbol{z}} = \tilde{\boldsymbol{S}}^{\dagger}\tilde{\boldsymbol{x}} = \left(\tilde{\boldsymbol{S}}^T\tilde{\boldsymbol{S}}\right)^{-1}\left(\tilde{\boldsymbol{S}}^T\tilde{\boldsymbol{x}}\right) = \left(\boldsymbol{S}^T\boldsymbol{S} + \boldsymbol{C}^T\boldsymbol{C}\right)^{-1}\left(\boldsymbol{S}^T\boldsymbol{x}\right). \tag{7}$$

The effective separation system for each of the components can be rewritten as

$$\begin{aligned} \hat{\boldsymbol{x}}_1 &= \left\{[\boldsymbol{I}_{N_1\times N_1}\mathbf{o}_{N_1\times N_2}]\left(\boldsymbol{S}^T\boldsymbol{S} + \boldsymbol{C}^T\boldsymbol{C}\right)^{-1}\boldsymbol{S}^T\right\}(\boldsymbol{x}) \\ &= \boldsymbol{S}_1^{\dagger}(\boldsymbol{x}) \\ \hat{\boldsymbol{x}}_2 &= \left\{[\mathbf{o}_{N_2\times N_1}\boldsymbol{I}_{N_2\times N_2}]\left(\boldsymbol{S}^T\boldsymbol{S} + \boldsymbol{C}^T\boldsymbol{C}\right)^{-1}\boldsymbol{S}^T\right\}(\boldsymbol{x}) \\ &= \boldsymbol{S}_2^{\dagger}(\boldsymbol{x}) \end{aligned} \tag{8}$$

where the notation $\boldsymbol{S}^T$ stands for the matrix transpose of the matrix $\boldsymbol{S}$, $\tilde{\boldsymbol{S}}^\dagger$ stands for the least-squares left-inverse of the matrix $\tilde{\boldsymbol{S}}$ and $\boldsymbol{S}_1^\dagger$, $\boldsymbol{S}_2^\dagger$ are the effective MAS algorithm inverse systems for each component. Note that in the case where the component periods are identical, the $\mathrm{lcm}(N_1, N_2) = N_1 = N_2$. In this case, we would require $N_1$ extra constraints, and hence knowledge of one of the signal components.

### B. Energy Demodulation of the Components

The separated components are then demodulated into IF and IA information signals using the discrete *energy separation algorithm* (ESA) of [7]. Although in essence any other monocomponent demodulation algorithms could have been used for demodulation, the ESA is employed here on account of its simplicity, efficiency, low complexity, and its excellent instantaneous-adapting nature [7]. A comparison of the ESA versus the classic AM–FM demodulation method based on the analytic signal and Hilbert transform can be found in [38]. We assume that the separated signal components can be modeled as discrete-time monocomponent AM–FM signals of the form $x_i[n] = A_i[n]\cos(\int_0^n \Omega_i[k]dk + \theta_i)$, $i = 1, \cdots, M$. Then the discrete-time Teager–Kaiser energy operator $\Psi(x[n]) = x^2[n] - x[n+1]x[n-1]$ is applied to the components $x_i[n]$ and their discrete-time derivative approximations $y_i[n] = x_i[n] - x_i[n-1]$. Finally, the IF and IA information of each separated component are estimated via the DESA-1[3] algorithm [7]

$$\hat{\Omega}_i[n] = \cos^{-1}\left(1 - \frac{\Psi(y_i[n]) + \Psi(y_i[n+1])}{4\Psi(x_i[n])}\right) \qquad (9)$$

$$|\hat{A}_i[n]| = \sqrt{\frac{\Psi[x_i[n]]}{\sin^2(\hat{\Omega}_i)}}. \qquad (10)$$

The demodulation errors of the ESA algorithm are practically negligible for AM–FM signals with realistic values of modulation parameters, but they can be reduced further by using simple smoothing [38] of the energy signals before applying the ESA. The carrier frequency and mean amplitude of each component are estimated from the mean of IF and IA signal estimates over the finite time interval [0, $N-1$] of signal duration

$$\hat{\Omega}_{ci} = \frac{1}{N}\sum_{n=0}^{N-1}\hat{\Omega}_i[n]$$
$$\hat{A}_{ci} = \frac{1}{N}\sum_{n=0}^{N-1}|\hat{A}_i[n]|. \qquad (11)$$

### C. Estimation of Component Periodicities

The underlying assumption in the development of the PASED algorithm is the exact prior knowledge of the component periodicities. The problem of estimating the periodicities can be solved using the *double difference function* (DDF) algorithm proposed in [3]. The two-dimensional lag parameter space of two cascaded comb filters is exhaustively searched for a minimum of the DDF objective function [3] defined by

$$\mathrm{DDF}[n, L_1, L_2] = \sum_{m=0}^{L-1} |x[n+m] - x[n+m+L_1] - x[n+m+L_2] + x[n+m+L_1+L_2]| \qquad (12)$$

where $L$ is the duration of the analysis window, $n$ is the analysis point, and $L_1 \mathrm{and} L_2$ are the respective lag parameters of the cascaded comb filters. The coordinates of the minimum of the DDF objective function furnish estimates of the two periodicities sought. The symmetry of the DDF function in the lag parameters can be used to reduce the search space to half a quadrant [3]. If the components of the composite signal are truly periodic, then this algorithm is guaranteed to find both the component periods unless the periods happen to be equal or multiples of a common subharmonic [3]. The modular structure of the DDF algorithm allows easy extension to the case where $M > 2$ at the expense of increased complexity in the period search.

## III. Two-Component AM–FM Signals

### A. Performance of PASED Algorithm

Consider real-valued two-component sinusoidally modulated AM–FM signals of the form

$$x[n] = \sum_{i=1}^{2} A_i[n]\cos\left(\int_0^n \Omega_i[m]dm + \theta_i\right) \qquad (13)$$

where the IF and IA information signals are sinusoidal

$$\Omega_i[n] = \Omega_{ci} + \Omega_{mi}\cos(\Omega_{fi}n + \beta_i)$$
$$A_i[n] = A_{ci}[1 + \kappa_i\cos(\Omega_{ai}n + \zeta_i)], \qquad \text{with } i = 1, 2. \quad (14)$$

Before discussing the performance of the PASED algorithm on the above signals, some performance related parameters need to be defined. A measure of the spectral separation between the components is the *normalized carrier separation* (NCS) parameter of the mixture defined by

$$\mathrm{NCS} = \frac{|\Omega_{c2} - \Omega_{c1}|}{\sum_{i=1}^{i=2}(\Omega_{mi} + \Omega_{fi} + \Omega_{ai})}. \qquad (15)$$

Note that the denominator is the Carson[4] bandwidth of the signal, which is a conservative estimate of the actual bandwidth [40]. The *mean power ratio* (MPR) parameter of the mixture is defined as

$$\mathrm{MPR\ (dB)} = 20\log\left(\frac{\sigma_{x1}}{\sigma_{x2}}\right) \qquad (16)$$

where $\sigma_{xi}$ is the RMS value of component $x_i[n]$, and measures the strength of the first component relative to the second. The strength of amplitude and frequency modulations with respect

[3]If, due to noise or modeling errors, the argument of the $\cos^{-1}(.)$ in (9) ever exceeds the range [$-1$, 1] at some isolated instants, then it is clipped to restrict it in [$-1$, 1] and to force the ESA estimate of IF to be in [0, $\pi$]. The number of such isolated instants is significantly reduced by smoothing the energy signals [38].

[4]The Carson bandwidth of this signal is the separation between the frequencies at which the spectral amplitudes are 1% of the carrier spectral amplitude when there is no modulation [40].

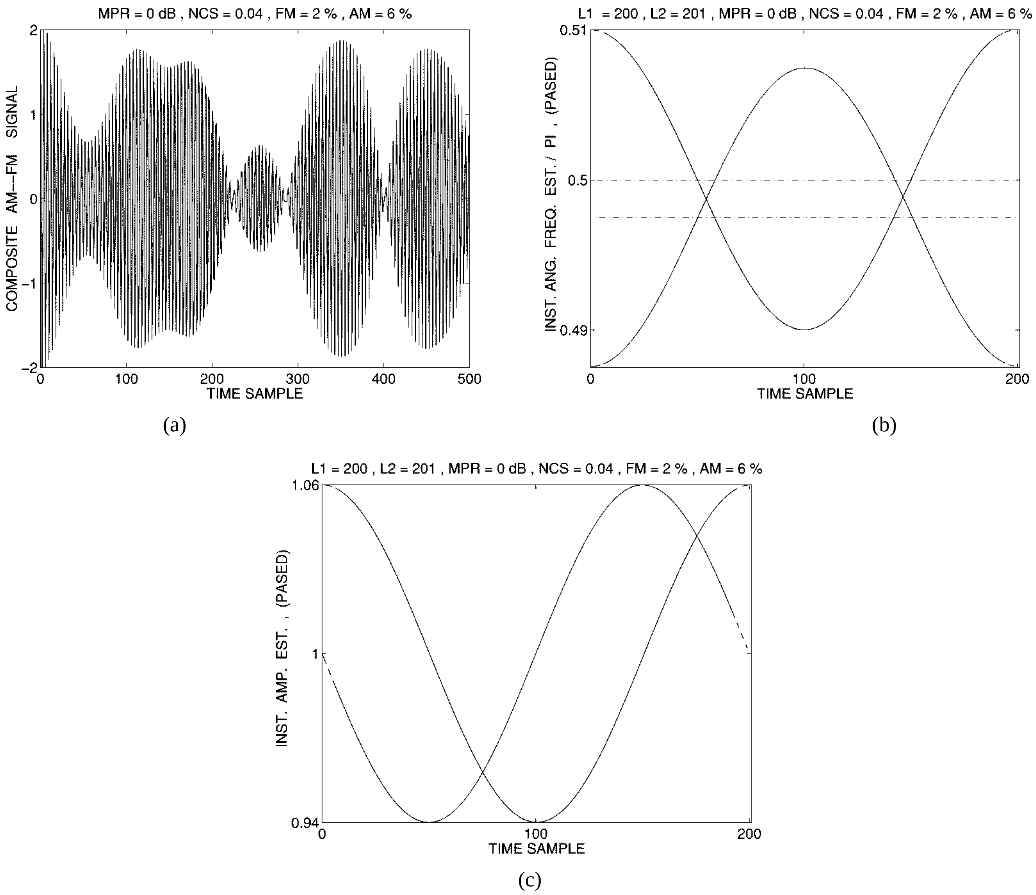


Fig. 3. Sinusoidal AM–FM example with coprime component periods. Sinusoidal AM–FM: (a) composite AM–FM signal, (b) IF and carrier estimates of the PASED algorithm (as fractions of $\pi$), and (c) IA estimates of the PASED algorithm, where solid lines show estimated signals, dashed lines show original signals, and dashed-dotted lines show estimated carrier frequencies. The IF signals are sinusoidal with 2% FM, 4% NCS and coprime component periods. The IA signals are also sinusoidal with 6% AM and an MPR of 0 dB.

to the carrier are measured by the AM amount $\kappa_i$ and the FM amount $(\Omega_{mi}/\Omega_{ci})$, both expressed as percentages. The *carrier to information bandwidth ratio* (CR/IB) of each component is defined as

$$(\mathrm{CR/IB})_i = \frac{\Omega_{ci}}{\max(\Omega_{fi},\, \Omega_{ai})} \tag{17}$$

and is a measure of how fast the signal modulations vary with respect to the carrier. This ratio is typically in the order $O(10)$ for speech resonances and in the order of $O(10^2)$ for AM radio and $O(10^3 - 10^4)$ for FM radio. Finally, the capability of various algorithms to track the signal modulations can be measured by the norms of the demodulation error. For example, the carrier-biased *normalized RMS error* (NRMSE) and *mean absolute error* (NMAE) associated with the demodulation are defined by

$$\mathrm{NRMSE} = \frac{||\Theta - \hat{\Theta}||_2}{||\Theta||_2}, \qquad \mathrm{NMAE} = \frac{||\Theta - \hat{\Theta}||_1}{||\Theta||_1} \tag{18}$$

where $\Theta$ represents the original IA or IF signal, $\hat{\Theta}$ is its estimate, and the notation $||.||_{1,\,2}$ stands for the $l_1$ or $l_2$ vector norms. The unbiased demodulation errors are defined similarly but with the carrier frequency and mean amplitude subtracted off from the IF and IA estimates.

When applying the PASED algorithm to two-component AM–FM signals, the components are modeled as quasiperiodic signals. Specifically, when the two IF and IA signals are sinusoidal, the quantities $L_i = \mathrm{lcm}(2\pi r/\Omega_{fi},\, 2\pi/\Omega_{ai})$, where $r$ is the smallest integer that makes the quantity $(\mathrm{CR/IB})_i r$ an integer, play the roles of the component periods.[5] For the examples in this paper, where $\Omega_{fi} = \Omega_{ai}$, $r = 1$, this expression reduces to $L_i = 2\pi/\Omega_{fi}$. The case where the IF signals are not sinusoidal is addressed later in this section. As an example, consider a two-component sinusoidally modulated AM–FM signal described by the composite signal in Fig. 3(a). The demodulation lengths of the two components are $L_1 = 200$ and $L_2 = 201$ and they are mutually prime. Since we are dealing with narrow-band bandpass components, the dc value of the first component can be approximated as zero. The IF estimates of the PASED algorithm are shown in Fig. 3(b), while the IA estimates of the proposed algorithm are shown in Fig. 3(c).

[5]This expression is based on the observation that if the signals $x[n] = A[n]$ and $y[n] = \cos(\phi[n])$ are periodic with fundamental periods $N_x$ and $N_y$ then $N = \mathrm{lcm}(N_x,\, N_y)$ is a period of their product but not necessarily the fundamental period and also on the observation that the component phase signal $\phi_i[n]$ will be periodic with period $N_{\phi_i} = 2\pi r/\Omega_{fi}$ only when the carrier frequency ramp signal $z_i[n] = \Omega_{ci} n$ is periodically extended with the same period.

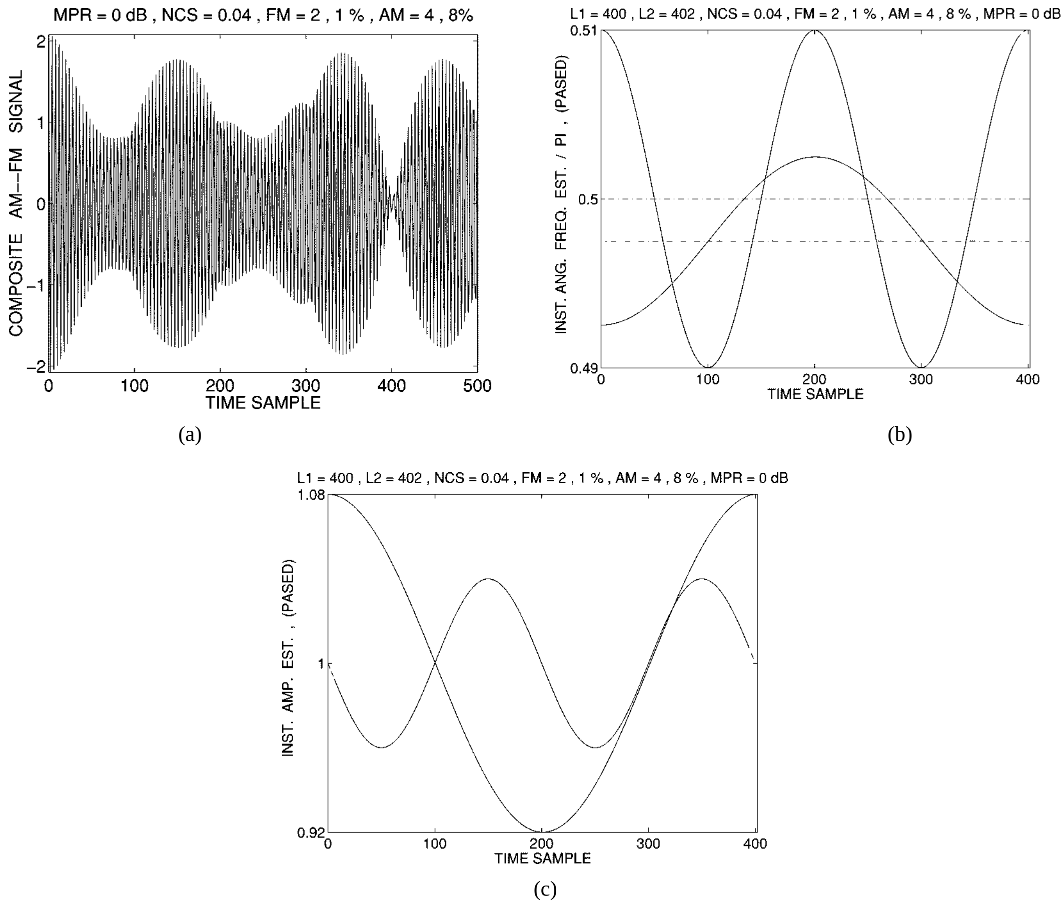


Fig. 4. Sinusoidal AM–FM example with noncoprime component periods. Noncoprime component periods: (a) composite AM–FM signal, (b) angular frequency estimates of PASED algorithm (as fractions of $\pi$), and (c) IA estimates of the PASED algorithm, where solid lines show estimated signals, dashed lines show original signals, and dashed-dotted lines show estimated carrier frequencies. The IF signals are sinusoidal with 2, 1% FM, respectively, with 4% NCS and noncoprime component periods. The IA signals are also sinusoidal with 4, 8% AM and an MPR of 0 dB.

When the component periods are not coprime then more dc value constraints are needed to complete the basic separation system. The angular frequency estimates and the IA estimates of the PASED algorithm for the signal environment shown in Fig. 4(a) are shown in Fig. 4(b) and (c). The demodulation lengths of the components in this case are $L_1 = 400$ and $L_2 = 402$ samples, respectively. As evident from Figs. 3 and 4, the frequency and amplitude demodulation errors of PASED algorithm are negligible since the estimated signals are almost indistinguishable from the originals even when the carrier frequencies are very close or the when the component IF tracks cross-over.

For AM–FM signals in AWGN, the denoising capability of the least-squares system in (6) enables simultaneous smoothing and demodulation. Consider the noisy FM signal described in Fig. 5(a). Period estimation for the noisy example, where the SNR is 30 dB, is shown in Fig. 5(b). The actual component periods are $N_1 = 200$ and $N_2 = 202$ samples while the estimated periods from the DDF image intensity plot are $\hat{N}_1 = 200$ and $\hat{N}_2 = 202$ samples. The energy signals in the ESA section of the algorithm are further smoothed using a 4-time application of binomial smoothing. The angular frequency estimates of the PASED algorithm are shown in Fig. 5(c). The carrier-unbiased frequency demodulation errors for the two components are 4% and 3.85%. The strength of the signal modulations can be increased to combat the presence of noise, but increase beyond a certain strength will produce more demodulation error due to loss of stationary behavior.

The ideas described above also apply when the component AM–FM signals have nonsinusoidal or even aperiodic IF signals. In such cases, following the analysis in [7], we assume knowledge of each AM–FM component signal over a finite time interval $[0, N_i - 1]$. Then, assuming periodic extension of the component outside this finite interval, each component IF signal can be expressed via the DFT as a finite discrete Fourier series of the form

$$\Omega[n] = \Omega_c + \sum_{k=1}^{K} \Omega_{mk} \cos(\Omega_{fk} n + \theta_k) \tag{19}$$

where $K < N/2$ and the carrier frequency is the dc term in the series

$$\Omega_c = \frac{1}{N} \sum_{n=0}^{N-1} \Omega[n].$$

In such cases, we set the required demodulation lengths $L_i$ equal to the periods $N_i$ of the extended signal components. As an example, consider a two-component AM–FM signal whose FM

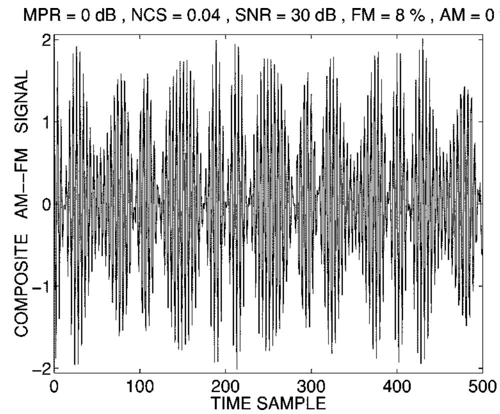


(a)

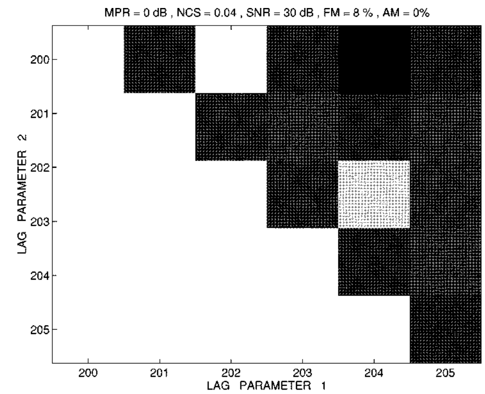


(b)

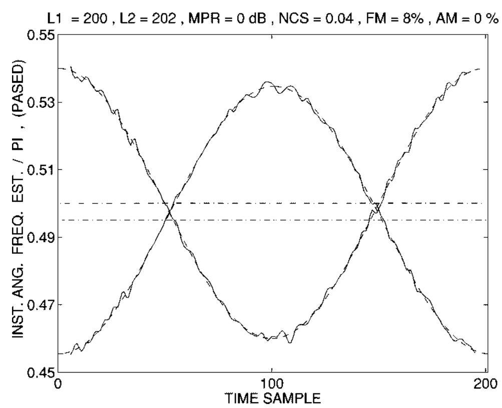


(c)

Fig. 5. Noisy AM–FM signal example with a SNR of 30 dB. Noisy example: (a) composite signal, (b) DDF over a half-quadrant search region, where dark areas indicate high DDF value and light areas indicate small DDF values, and (c) angular frequency estimates (as fractions of $\pi$). The SNR of the signal mixture is 30 dB. 4-time binomial smoothing was used for smoothing the energy signals in the ESA. The IF signals are sinusoidal with 8% FM, with 4% NCS.

parts are chirped, i.e., FM with aperiodic linear IF signals. Over finite intervals the two IF signals are

$$\Omega_1[n] = \frac{\pi}{2} + \frac{\pi}{400}\left(\frac{2n}{399} - 1\right), \qquad 0 \le n \le 399$$

$$\Omega_2[n] = \frac{\pi}{2.005} - \frac{\pi}{400}\left(\frac{2n}{400} - 1\right), \qquad 0 \le n \le 400.$$

The IA signals of this example are sinusoidal with 6% amplitude modulation, with a CR/IB of 50, NCS of 0.04, and an MPR of 0 dB. The demodulation lengths used in this example were $L_1 = 400$ and $L_2 = 401$. The composite signal of the example is shown in Fig. 6(a), the angular frequency estimates of the PASED algorithm are shown in Fig. 6(b) and the IA estimates of the PASED algorithm are shown in Fig. 6(c). Again, the PASED algorithm performs very well both in the challenging cochannel range and in the case where the component IF tracks cross each other.

## IV. Comparison of the Demodulation Algorithms

Previously investigated techniques for multicomponent AM–FM signal separation and demodulation either assume that the components of the signal are distinct ridges [1] in the time-frequency plane or that the components are separable via linear time invariant filtering techniques. For signals in the cochannel range, i.e., when $\mathrm{NCS} < 0.2$, these assumptions do not hold causing a break down in these algorithms. For the purpose of comparing the algorithms, the effect of the NCS and MPR parameters on demodulation on these algorithms is studied using two-component sinusoidally modulated AM–FM signals.

Demodulation algorithms like the LMS algorithm, the RLS algorithm, and the CC-DPLL algorithm are highly parameter dependent. The performance, the stability, and the noise suppression capabilities of the LMS and the RLS algorithms are dependent on the choice of the adaptive step size parameter $\mu$ or the memory factor $\rho$, while the performance and the stability of the CC-DPLL algorithm is dependent on the choice of loop filter parameters.

Fig. 7 describes a two-component sinusoidally modulated AM–FM example where the PASED, the LMS (normalized version of the LMS [30]), the exponentially-weighted RLS, the HRR, the EKF, the MESA, and the CC-DPLL algorithms are compared for a fixed parameter set with $\mathrm{NCS} = 1$ and $\mathrm{MPR} = 0$ dB. Fourth-order predictors ($P = 4$) are used in the case of the adaptive algorithms with a step size parameter of $\mu = 1.25$ for the normalized LMS [30] and a exponential weight parameter of $\rho = 0.945$ for the RLS algorithm [29]. A Hankel order of $c = 20$ is used in the HRR algorithm [32]. First-order loop filters are used in the design of the

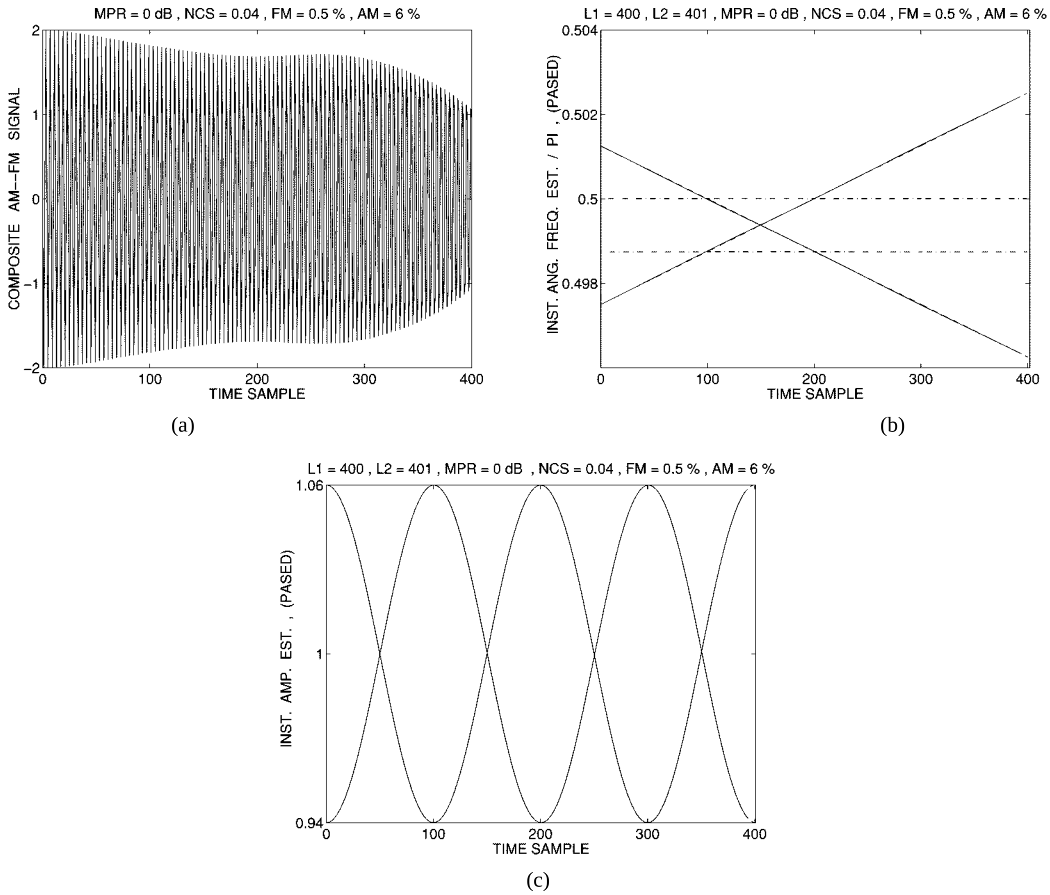


Fig. 6. Linear-FM and sinusoidal-AM example. Chirp example: (a) composite signal, (b) angular frequency estimates of the PASED algorithm (as fractions of $\pi$), and (c) IA estimates of the PASED algorithm. Solid lines here indicate estimates, dashed lines indicate actual quantities and dashed-dotted lines are carrier frequency estimates. The component IF signals are linear with 0.5% FM and mutually coprime component periods with a NCS of ≈4%, while the IA signals are sinusoidal with an MPR parameter of 0 dB and 6% AM.

CC-DPLL so that the closed-loop system is second-order with a damping ratio of 0.707. Linear-phase FIR multiband filters designed using the Kaiser window method [14] for an order of $L = 350$ with $\beta = 6.65$, which is a parameter related to the passband tolerance of the filters, are used in the MESA [5]. The components of the signal in this case have significant spectral overlap as shown in Fig. 7(b). For this spectral separation, the LMS algorithm exhibits severe beating in the estimates as shown in Fig. 7(d), the RLS estimates in Fig. 7(e) also are severely distorted, and post-smoothing of the IF estimates does not reduce the frequency demodulation error significantly. The carrier unbiased frequency estimates of the PASED and the other algorithms are shown in Fig. 7(a)–(h). The percentage NRMSE's of the proposed PASED algorithm are two orders less than the others as described in Fig. 7(j).

### A. Effect of Spectral Separation (NCS Parameter)

In the definition of multicomponent AM–FM signal model it has been assumed that the components are distinct in the time-frequency planesanth7a.tif. The challenging case, however, is the cochannel case where the components of the signal overlap spectrally. In this case the components are no longer distinct and interact with each other. This interaction for the case of two-component continuous-time sinusoidal signals of the form

$$x(t) = a_1 \cos(\omega_1 t + \theta_1) + a_2 \cos(\omega_2 t + \theta_2)$$

is embodied in the instantaneous envelope and the frequency of the composite signal [2]

$$\begin{aligned}|a(t)| &= \left[a_1^2 + a_2^2 + 2a_1 a_2 \cos\left((\omega_2 - \omega_1)t + \theta_1 - \theta_2\right)\right]^{1/2}\\ \omega(t) &= \left(\frac{\omega_1 + \omega_2}{2}\right) + \left(\frac{\omega_1 - \omega_2}{2}\right)\left(\frac{a_2^2 - a_1^2}{|a(t)|^2}\right). \end{aligned} \tag{20}$$

Decrease in the NCS parameter produces singularity problems in these algorithms:

- The energy equations of the EDM algorithm become ill-conditioned [11].
- The covariance matrices used in the LMS algorithm, the RLS algorithm, and the MUSIC algorithm become ill-conditioned [8].
- The Fisher information matrix used in the maximum likelihood methods [33] becomes ill-conditioned.
- The Toeplitz and the Hankel matrix systems of the ITD and HRR algorithms become ill-conditioned.

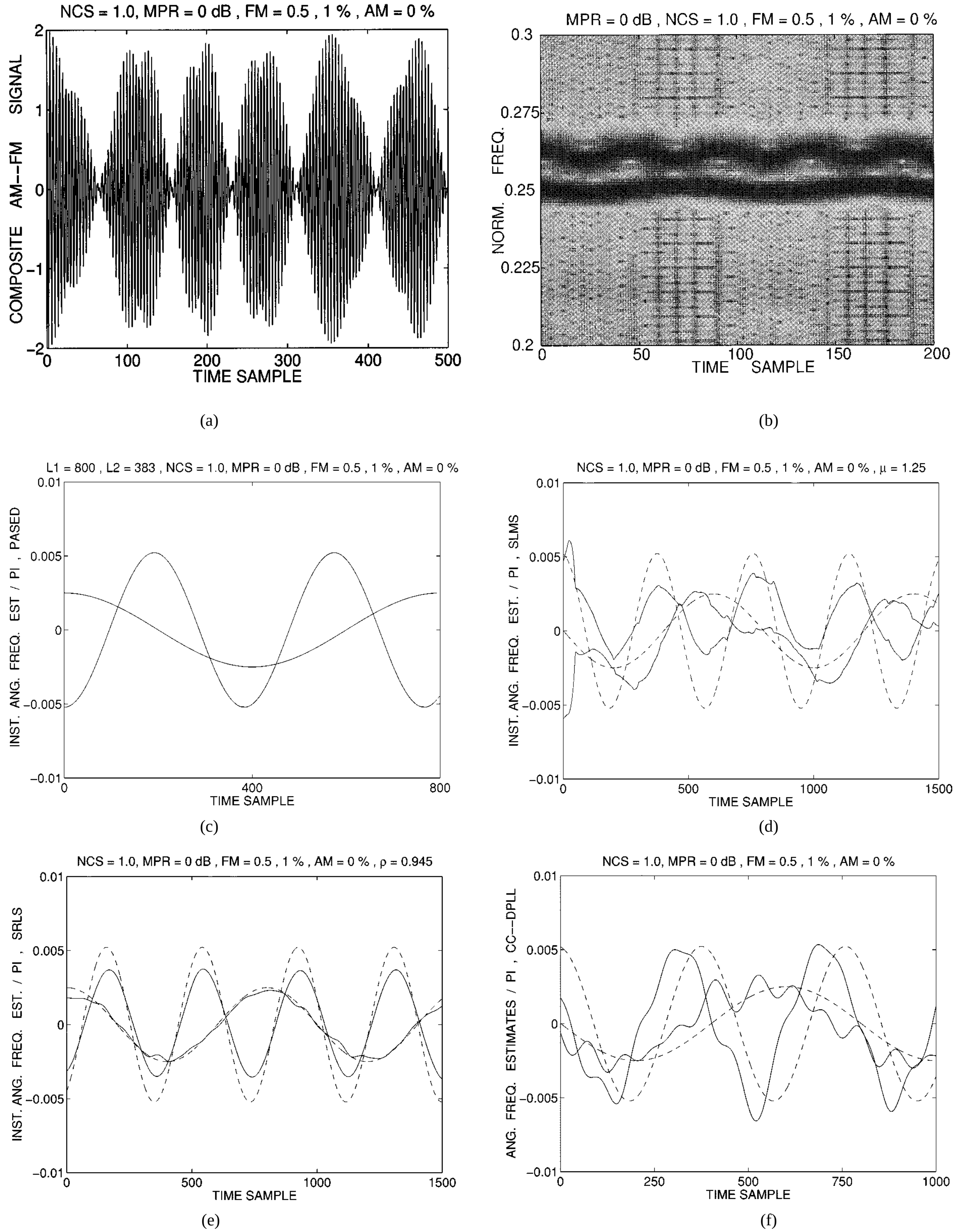


Fig. 7. Comparison of the PASED algorithm with other multicomponent AM–FM demodulation algorithms. (a) Composite FM signal. (b) Spectrogram of the composite signal using a Hamming window of 384 samples and an FFT of 1024 samples with a time-increment of eight samples. (c) Carrier-unbiased angular IF estimates of the PASED algorithm. (d), (e) Estimates of the SLMS and the SRLS algorithm. (f) Estimates of the CC-DPLL algorithm using a first-order loop filter. Solid lines are the estimates and the dashed lines are the actual quantities. Post-smoothing of the IF estimates using moving average and 9-pt median filtering removes some of the interference and spikes but at the cost of distorting the IF estimates.

- The observability Gramian of the two-component state model in the CC-DPLL and the EKF algorithms become ill-conditioned [21], [23].

The interaction between the components manifests itself as beating in the estimates. Post-smoothing of the estimates can alleviate this problem to a certain extent. The demodulation

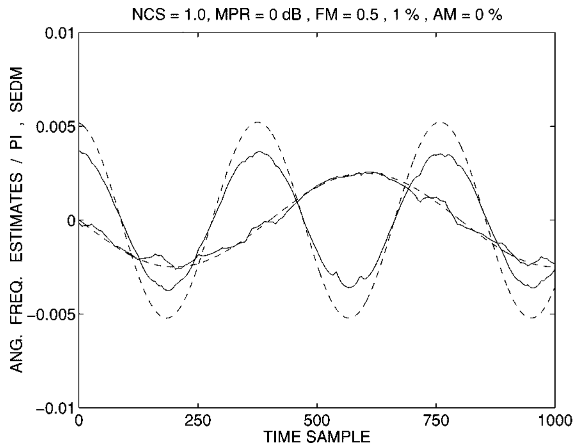


(g)

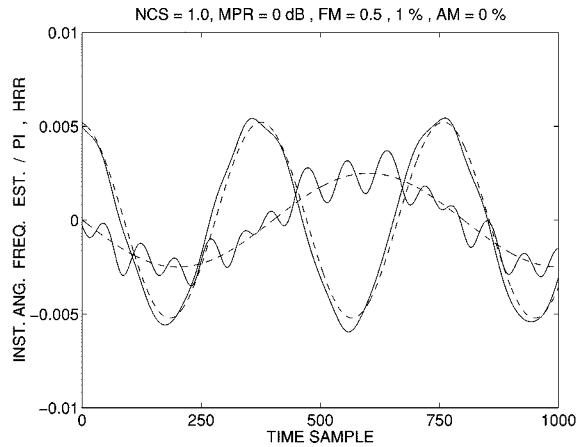


(h)

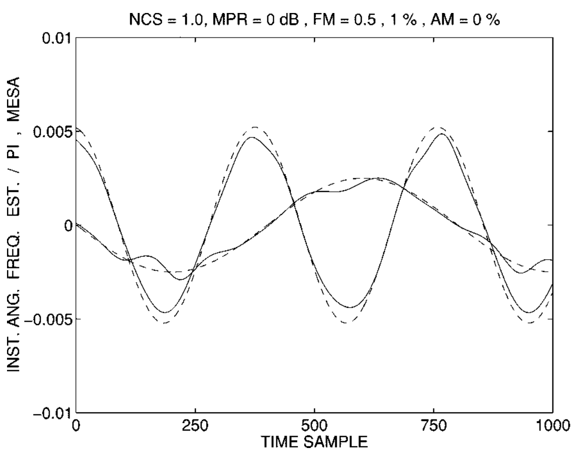


(i)

| **Algorithm** | **NRMSE$_1$ (%)** | **NRMSE$_2$ (%)** |
|---|---|---|
| **PASED** | 0.01 | 0.08 |
| **MESA** | 13.96 | 13.88 |
| **HRR** | 38.1 | 14.93 |
| **SLMS** | 73.3 | 63.25 |
| **SRLS** | 56.04 | 38.77 |
| **CC-DPLL** | 23.9 | 15.3 |
| **SEDM** | 16.6 | 31.84 |

(j)

Fig. 7. (*Continued.*) Comparison of the PASED algorithm with other multicomponent AM–FM demodulation algorithms. (g), (h) Corresponding estimates of the SEDM and the HRR algorithms, respectively. Solid lines are the estimates and the dashed lines are the actual quantities. Post-smoothing of the IF estimates using moving average and 9-pt median filtering removes some of the interference and spikes but at the cost of distorting the IF estimates.

algorithm $X$ with post-smoothing is referred to as $SX$, i.e., the EDM algorithm with post-smoothing is referred to as the SEDM algorithm. Post-smoothing of the estimates using 9-point median filtering and moving average filtering of the GDE coefficients (slow time-varying quantities) and the estimates in the EDM removes a significant amount of the interference but in the case of sinusoidal modulation fails for NCS parameters less than one. The EDM algorithm, particularly for voice modulated FM applications, can provide intelligible estimates for separations down to 25% of the RF bandwidth but fails for further decrease in the NCS parameter.

The proposed PASED algorithm, on the other hand, does not make any assumption about the spectral location of the components. This enables the algorithm to handle the case when the components of the signal overlap spectrally and the case where the IF tracks cross-over where all the existing techniques fail. Fig. 8(a) illustrates the effect of the NCS parameter on the different algorithms. Note that the performance of the PASED algorithm is independent of the NCS parameter.

State flipping occurs in the CC-DPLL algorithm, i.e., the condition where the DPLL's lock onto the wrong signal, as a consequence of unobservability of the states of the state-model. This situation is conditioned on the following: 1) frequency equality, i.e., when the IF tracks cross-over; 2) components completely in phase or out of phase; or 3) identical component state transition matrices [23]. The PASED algorithm, on the other hand, does not exhibit this phenomenon and is capable of handling the case where the component IF tracks cross.

### B. Effect of the Mean Power Ratio (MPR) Parameter

The MPR parameter of the signal mixture is a measure of the strength of the desired signal relative to the interference and is also a measure of the strength of the interaction between the components. For large MPR parameters, the stronger component dominates the signal mixture and the interaction between the components is less. The covariance matrix for the multicomponent demodulation problem when one of the components is stronger than the other becomes singular, and, consequently, demodulation algorithms like the LMS develop singularities as the MPR parameter increases [30]. The performance of the CC-DPLL and the EKF algorithms can be characterized by the observability Gramian of the state-space model for the composite signal [23]. As one of the components becomes more powerful than the other, the lower-power component becomes less observable resulting in increased error covariance due to an

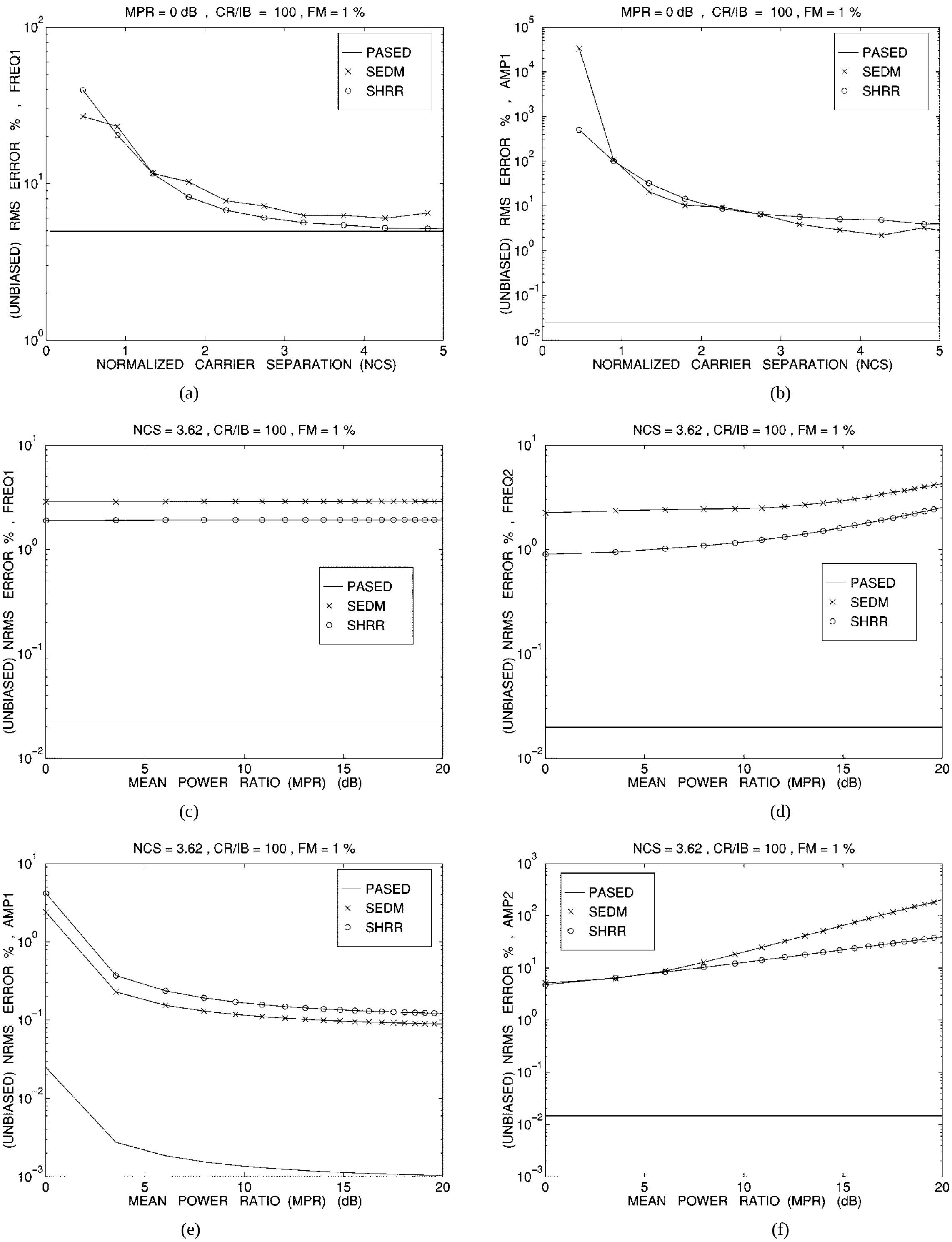


Fig. 8. Effect of NCS and MPR parameters on demodulation in the PASED, the SEDM, and the SHRR algorithms. (a), (b) Effect of NCS on frequency and amplitude demodulation in the PASED, the SEDM, and the SHRR algorithms (the other algorithms developed singularities and broke down for $\mathrm{NCS} < 0.5$) and (c)–(f) effect of the MPR parameter on frequency and amplitude demodulation in the PASED, the SEDM, and the SHRR algorithms. Amplitude estimation in the SHRR is accomplished by integrating the IF estimates and solving a least-squares system for the amplitudes. All curves were obtained by averaging over $\kappa_i \in [1-10]$% AM. The notation $SX$ refers to the algorithm $X$ with post-smoothing.

increase in the coupling between the DPLL's and an increase in the demodulation error corresponding to the weaker component [22], [23].

The frequency estimation section of the EDM algorithm is obtained from the GDE of the composite signal invariant to the amplitudes [39]. Consequently, frequency demodulation in the EDM is independent of the MPR parameter. The amplitude demodulation section of the EDM is, however, adversely affected by an increase in the MPR parameter. As the MPR increases, the relative strength of the first component with respect to the second component increases with a corresponding decrease in the amplitude demodulation error of the first component and an

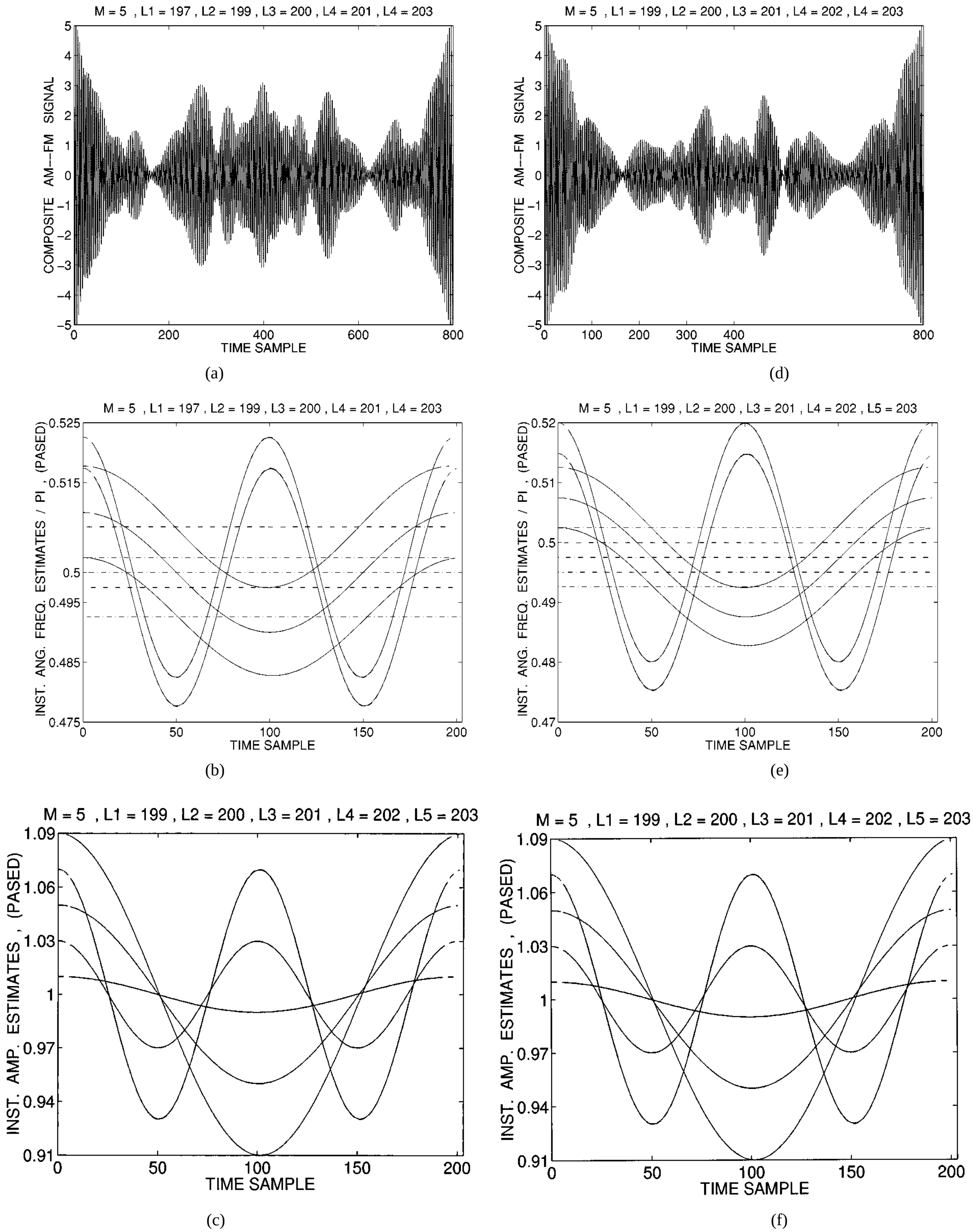


Fig. 9. Five-component example with both pairwise coprime and pairwise noncoprime component periods. (a), (d) Composite AM–FM signal. (b), (e) Angular frequency estimates of the multicomponent-PASED algorithm (as fractions of $\pi$). (c), (f) IA estimates of the components via the multicomponent-PASED algorithm. Solid lines are estimates, dashed lines are actual quantities and dashed-dotted lines are carrier frequency estimates. The IF signals are sinusoidal with {2, 4, 2, 4, 2}% FM. The IA signals are also sinusoidal with $\kappa_i \in$ {1, 3, 5, 7, 9}% AM.

increase in the demodulation error of the second, weaker component [11].

The proposed PASED algorithm, however, does not make any assumptions regarding the component interaction, and frequency demodulation in the PASED algorithm is independent of the MPR parameter. An increase in the power of one of the components with respect to the other results in a decrease in the amplitude demodulation error of the stronger component but has no effect on the demodulation error of the weaker one. The effect of the MPR parameter on frequency and amplitude demodulation in the PASED, the SEDM, and the SHRR algorithms is shown in Fig. 8(c)–(f).

## V. Multicomponent PASED Algorithm

The $M$-component PASED algorithm is based on the same philosophy as that of the two-component problem. The separation matrix $\boldsymbol{S}_M$ has $M$ circulant blocks instead of just two

$$\underbrace{\begin{pmatrix} x[0] \\ x[1] \\ \vdots \\ x[N-1] \end{pmatrix}}_{\boldsymbol{x}} = \underbrace{\begin{pmatrix} \boldsymbol{I}_{N_1} & \boldsymbol{I}_{N_2} & \cdots & \boldsymbol{I}_{N_M} \\ \boldsymbol{I}_{N_1} & \boldsymbol{I}_{N_2} & \cdots & \boldsymbol{I}_{N_M} \\ \vdots & \vdots & \vdots & \end{pmatrix}}_{\boldsymbol{S}_M} \underbrace{\begin{pmatrix} \boldsymbol{x}_1 \\ \boldsymbol{x}_2 \\ \vdots \\ \boldsymbol{x}_M \end{pmatrix}}_{\boldsymbol{z}}. \tag{21}$$

The rank of the $M$-component separation matrix $r(\boldsymbol{S}_M)$ is (proof given in Appendix A)

$$\begin{aligned} r(\boldsymbol{S}_M) &= \sum_{i=1}^{M} N_i - (M-1)\gcd(N_1, N_2, \cdots, N_M), \\ &\qquad \prod_{i,j,i\neq j} \gcd(N_i, N_j) = 1 \text{ or } M = 2 \\ r(\boldsymbol{S}_M) &\geq \sum_{i=1}^{M} N_i - \sum_{i,j,i<j} \gcd(N_i, N_j), \\ &\qquad \text{otherwise.} \end{aligned} \tag{22}$$

The rank of the separation system in the multicomponent case now depends on the pairwise component interactions which are embodied in the form of the product of the pairwise gcd's. For the first case, the extra constraints, as in the two-component case, are obtained as dc value constraints on the $(M-1)$ narrow-band bandpass components at their original scale as

$$\sum_{n=0}^{N_i-1} x_i[n] = 0, \qquad i = 1, 2, \cdots, (M-1). \tag{23}$$

For the second case, extra constraints are needed and are obtained by considering the two-component interactions in the composite signal. For an $M$ component signal, there are $\binom{M}{2}$ possible two-component interactions. The constraints in this case are obtained from the dc value constraints applied to the interactions using the information on the pairwise $\gcd R_{ij} = \gcd(N_i, N_j), i < j$. For the interaction between the $(i, j)$ pair of components, the constraints take the form

$$\begin{aligned} &\sum_{n=0}^{(N_i/R_{ij})-1} x_i[R_{ij}n + p] + \sum_{n=0}^{(N_j/R_{ij})-1} x_j[R_{ij}n + p] = 0, \\ &\quad 1 \leq i < j \leq M, \quad 0 \leq p \leq R_{ij} - 1. \end{aligned} \tag{24}$$

The number of constraints and extra information needed goes up with an increase in the number of signal components and the gcd. As an example consider the case of a five-component sinusoidally modulated AM–FM signal where the component periods are pairwise coprime. The composite signal of the example is shown in Fig. 9(a). The angular frequency estimates of the multicomponent-PASED algorithm are shown in Fig. 9(b) and the IA estimates of the multicomponent-PASED algorithm are shown in Fig. 9(c). The IF's of the components overlap indicating that the components overlap spectrally. As in the two-component case, with $\Omega_{fi} = \Omega_{ai}$, $r = 1$, the demodulation lengths of the PASED algorithm become $L_i = 2\pi/\Omega_{fi}$, $i = 1, 2, \cdots, M$. The minimum number of composite signal samples needed is $\sum_i L_i$.

Fig. 9(d)–(f) shows another five-component example where the component periods are coprime overall but not pairwise coprime. Fig. 9(a)–(f) describes the excellent performance of PASED algorithm on demodulating multicomponent AM–FM signals even when the components have complete spectral overlap and the IF signals frequently cross over. Alternatively, the $M$ component separation problem can be treated as a sequence of two-component separation problems [12], [15]

$$\begin{aligned} x[n] &= \sum_{i=1}^{M} x_i[n] = x_1[n] + \underbrace{\sum_{i=2}^{M} x_i[n]}_{\tilde{x}_2[n]} \\ &= x_1[n] + x_2[n] + \underbrace{\sum_{i=3}^{M} x_i[n]}_{\tilde{x}_3[n]}. \end{aligned}$$

This method, however, requires the use of $N_1 + \mathrm{lcm}(N_2, N_3, \cdots, N_M)$ samples of the composite signal for separation (assuming no spectral cancellation) while the proposed PASED algorithm requires $\sum_i N_i$ composite signal samples.

## VI. Discussion

### A. Application to Cohannel and Adjacent Channel Separation

The denominator of the NCS parameter defined in (15) is the Carson bandwidth of the AM–FM signal which is a conservative estimate of the actual bandwidth of the signal. It is therefore more appropriate in voice-modulated FM applications to use the RF bandwidth of the signal to compute the NCS parameter. With the RF bandwidth as the normalization factor: NCS parameters $> 1$ indicate that the components are well separated and distinct, $\mathrm{NCS} = 1$ indicates that components are touching each other and when NCS parameter $< 1$ the components start to overlap and interact. For spectral separations in the cochannel range, i.e., NCS parameter $< 0.1$, the components overlap completely.

Among the existing multicomponent algorithms, the EDM algorithm has the advantages of computational simplicity and excellent time-resolution while experiencing similar limitations in the spectral separations it can handle as mostother existing algorithms [11]. In particular, when applied to the problem of demodulating voice-modulated two-component FM signals, the EDM algorithm has the capability of providing intelligible message estimates for spectral separations up to 25% of the RF bandwidth, but breaks down for further decrease in spectral separation. In the cochannel region all of the existing techniques develop singularity problems. The proposed PASED algorithm, however, does not assume that the components need to be distinct and is not affected by a decrease in spectral separation.

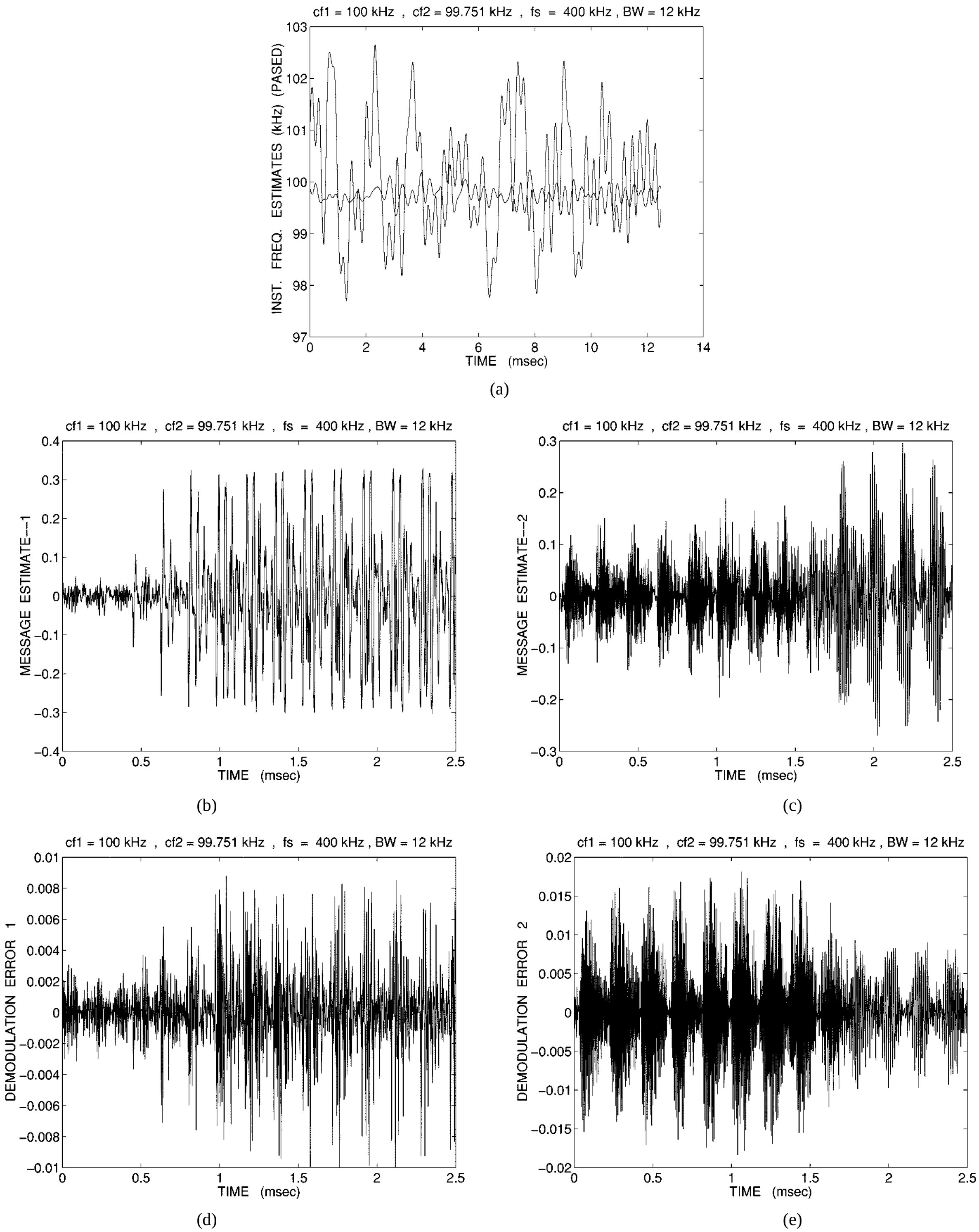


Fig. 10. PASED-based separation and demodulation of voice-modulated cochannel FM signals. (a) Instantaneous frequency estimates of the PASED. (b), (c) Demodulated message signals of the PASED. (d), (e) Associated demodulation errors of the PASED.

Some of the adaptive techniques like the LMS algorithm are also sensitive to the *relative power ratio* (MPR) of the components and develop singularity problems when the ratio is high. The performance of the proposed PASED algorithm is independent of the MPR parameter.

An example of applying the PASED algorithm to the problem of separation and demodulation of two-component voice-modulated FM signals is shown in Fig. 10, where the components overlap spectrally, i.e., the cochannel range. The sampling period of the message signals is $f_s = 400$ kHz, and the carrier frequencies of the components are $f_{ci} = 100,\ 99.75$ kHz. The RF bandwidth of each component is 12 kHz and the components are modulated with 6% FM. With these parameters, the IF's of the components overlap indicating significant spectral overlap. Actually, the carrier separation is 2% of the RF bandwidth (NCS = 0.02). The IF estimates of the example are shown in Fig. 10(a). The demodulated message signals of the PASED are shown in Fig. 10(b) and (c) and the corresponding demodulation errors are shown in Fig. 10(d) and (e).

## APPENDIX

### A. Pairwise Coprime Periods

*Theorem 1:* The $M$-component separation matrix $\boldsymbol{S}_M$ in the case where the component periods $\{N_i,\, i = 1, 2, \cdots, M\}$ are pairwise coprime or if there are only two-components, is of rank

$$r(\boldsymbol{S}_M) = \sum_{i=1}^{M} N_i - (M-1)\gcd(N_1, N_2 \cdots, N_M), \qquad \prod_{i,j,i\neq j} \gcd(N_i, N_j) = 1 \text{ or } M = 2.$$

*Proof:* The $M$-component separation matrix $\boldsymbol{S}_M$ has $(\sum_{i=1}^{M} N_i)$ columns and, hence, a maximum possible column rank of

$$r_{\max} = \sum_{i=1}^{M} N_i. \tag{25}$$

Exploiting the periodicity of the components we have

$$x_i[n] = x_i[n + N_i], \qquad i = 1, 2, \cdots M. \tag{26}$$

If $(M-1)$ initial values $x_i[0]$, $i = 2, \cdots M$, are known, using periodicity we can obtain $N_1$ samples of the first component using

$$x_1[n] = x[n] - (x_2[0] + x_3[0] \cdots + x_M[0]) \tag{27}$$

for the indices

$$n = R_{N_1}(k\,\mathrm{lcm}(N_2, \cdots, N_M)), \qquad 0 \le k \le (N_1 - 1) \tag{28}$$

where the notation $R_i(j)$ denotes the remainder of the integer $j$ modulo $i$ defined by $R_i(j) \equiv r(\mathrm{mod}\, i)$. The next step is to show that these indices are distinct and within the range of 0 and $N_1$. Let $A_1$ and $A_2$ be any two of these indices such that

$$\begin{aligned} A_1 &= M_1\,\mathrm{lcm}(N_2, N_3 \cdots, N_M) \equiv r_1(\mathrm{mod}\, N_1) \\ A_2 &= M_2\,\mathrm{lcm}(N_2, N_3 \cdots, N_M) \equiv r_2(\mathrm{mod}\, N_1) \end{aligned} \tag{29}$$

where $0 \le M_1 \ne M_2 \le N_1 - 1$. If the component periods are pairwise coprime then

$$\begin{aligned} \gcd(N_1, N_2, \cdots N_M) &= 1 \\ \mathrm{lcm}(N_1, N_2, \cdots N_M) &= \prod_{i=1}^{M} N_i \end{aligned} \tag{30}$$

and, hence

$$\begin{aligned} A_1 &= M_1 \prod_{i=2}^{M} N_i \equiv r_1(\mathrm{mod}\, N_1) \\ A_2 &= M_2 \prod_{i=2}^{M} N_i \equiv r_2(\mathrm{mod}\, N_1). \end{aligned} \tag{31}$$

Subtracting the indices and using the property of the modulo operator we have

$$A_1 - A_2 = (M_1 - M_2) \prod_{i=2}^{M} N_i \equiv (r_1 - r_2)(\mathrm{mod}\, N_1). \tag{32}$$

Since the component periods are pairwise coprime and $M_1 - M_2 < N_1$, this implies that the transformation from $A_i \leftrightarrow r_i(\mathrm{mod}\, N_1)$ is unique and that the indices are within the range of 0 and $N_1$. This implies that when the component periods are pairwise coprime and given that one has knowledge of $(M-1)$ initial values of the components other than the $i$th component, $N_i$ distinct samples of the $i$th component can be obtained from the basic separation system. This in turn implies that the rank of the $M$-component separation matrix, $\boldsymbol{S}_M$, which is also the number of linearly independent columns in the matrix $\boldsymbol{S}_M$, is

$$r(\boldsymbol{S}_M) = \sum_{i=1}^{M} N_i - (M-1), \qquad \prod_{i,j,i\neq j} \gcd(N_i, N_j) = 1.$$

For the two-component case, it has been shown [12], [15] that the rank of the two-component separation matrix

$$\begin{aligned} r(\boldsymbol{S}_2) &= N_1 + N_2 - \gcd(N_1, N_2) \\ r(N(\boldsymbol{S}_2)) &= \gcd(N_1, N_2). \end{aligned} \tag{33}$$

Combining these results we have that

$$r(\boldsymbol{S}_M) = \sum_{i=1}^{M} N_i - (M-1)\gcd(N_1, N_2 \cdots, N_M), \qquad \prod_{i,j,i\neq j} \gcd(N_i, N_j) = 1 \text{ or } M = 2.$$

In other words, "the solution to the algebraic separation system of the PASED algorithm in the case where the composite signal contains $M$ components whose periods are coprime is equivalent to the solution to the two-component case where there are $(M-1)$ two-point interactions as opposed to just one." The interaction pattern for the case where the component periods are not pairwise coprime contains $\binom{M}{k}$ $k$-point interactions embodied in the form of the appropriate gcd.

### B. General Case

*Theorem 2:* The rank of the $M$-component separation matrix $\boldsymbol{S}_M$, where the component periods are $\{N_i,\, i = 1, 2, \cdots, M,\, M \ge 2\}$ in the general case, is given by (33a), shown at the botttom of the following page.

*Proof:* As in the coprime case, the maximum possible rank for the matrix $\boldsymbol{S}_M$ is the column rank of the matrix $r_{\max} = \sum_{i=1}^{M} N_i$. The $n$ component separation matrix $\boldsymbol{S}_n$ can be written in block form

$$\boldsymbol{S}_n = [\boldsymbol{B}_1|\boldsymbol{B}_2|\cdots \boldsymbol{B}_n]$$

where the block $\boldsymbol{B}_i$ corresponds to blocks of identity matrices of order $N_i$ that correspond to the $i$th component. The rank of the $n$ component separation matrix, $r(\boldsymbol{S}_n)$, is the number of linearly independent column vectors in $\boldsymbol{S}_n$ and can be evaluated using subspace addition

$$r(\boldsymbol{S}_n) = \dim\left(\sum_{i=1}^{n} \text{span}(\boldsymbol{B}_i)\right). \tag{34}$$

Within each block $\boldsymbol{B}_i$, all the column vectors are linearly independent and orthogonal, hence

$$\dim(\text{span}(\boldsymbol{B}_i)) = N_i. \tag{35}$$

From the rank of the separation matrix in the two-component case as given by (33), the number of linearly dependent vectors, i.e., the dimension of the null space among the columns of any two blocks that are different put together is

$$\begin{aligned} r_{\max} &- r(\text{span}(\boldsymbol{B}_i) + \text{span}(\boldsymbol{B}_j)) \\ &= \dim\left(\text{span}(\boldsymbol{B}_i) \bigcap \text{span}(\boldsymbol{B}_j)\right) \\ &= \gcd(N_i, N_j), \qquad i \neq j. \end{aligned} \tag{36}$$

For the case of any two blocks put together, each column in the block $\boldsymbol{B}_i$ has ones alternating every $N_i$ slots. Similarly each column vector in the block $\boldsymbol{B}_j$ has ones alternating every $N_j$ slots. The block matrix that corresponds to the intersection of the spans of the two blocks therefore contains column vectors that have ones alternating every $R_{i,j} = \gcd(N_i, N_j)$ slots and can be written as

$$\left[\text{span}(\boldsymbol{B}_i) \bigcap \text{span}(\boldsymbol{B}_j)\right] = \begin{pmatrix} \boldsymbol{I}_{R_{i,j}} \\ \boldsymbol{I}_{R_{i,j}} \\ \vdots \end{pmatrix}. \tag{37}$$

The structure of the block matrix corresponding to the intersection of the spans of the blocks $\boldsymbol{B}_i$ and $\boldsymbol{B}_j$ is therefore identical to that of any of the other blocks $[\boldsymbol{B}_i, i = 1, 2, \cdots, n]$ (only the dimension, $R_{i,j}$, of the identity matrices is different). For the case of three arbitrary matrix blocks put together, the dimension of the intersection of the spans of the column of each block, consequently, is given by

$$\begin{aligned} \dim&\left(\bigcap_{i=1}^{3} \text{span}(\boldsymbol{B}_i)\right) \\ &= \dim\left(\left[\text{span}(\boldsymbol{B}_i) \bigcap \text{span}(\boldsymbol{B}_j)\right] \bigcap \text{span}(\boldsymbol{B}_k)\right) \\ &= \gcd[\gcd(N_i, N_j), N_k] \\ &= \gcd(N_i, N_j, N_k), \qquad i \neq j \neq k. \end{aligned} \tag{38}$$

This intersection of the spans of the blocks can be generalized as

$$\dim\left(\bigcap_{i=1}^{n} \text{span}(\boldsymbol{B}_i)\right) = \gcd(N_1, N_2, \cdots, N_n). \tag{39}$$

If $\{\boldsymbol{V}_i, i = 1, 2, \cdots, n\}$ is a sequence of subspaces in a finite dimensional vector space $\boldsymbol{V}$ then it can be shown for the case of $n = 2$ that [31]

$$\dim(\boldsymbol{V}_1 + \boldsymbol{V}_2) = \dim(\boldsymbol{V}_1) + \dim(\boldsymbol{V}_2) - \dim\left(\boldsymbol{V}_1 \bigcap \boldsymbol{V}_2\right). \tag{40}$$

This can further be extended through mathematical induction to the case of $n$ components as

$$\begin{aligned} \dim\left(\sum_{i=1}^{n} \boldsymbol{V}_i\right) = &\sum_{i=1}^{n} \dim(\boldsymbol{V}_i) - \sum_{i,j,i<j} \dim\left(\boldsymbol{V}_i \bigcap \boldsymbol{V}_j\right) \\ &+ \sum_{i,j,k,i<j<k} \dim\left(\boldsymbol{V}_i \bigcap \boldsymbol{V}_j \bigcap \boldsymbol{V}_k\right) \\ &+ \cdots (-1)^{n-1} \dim\left(\bigcap_{i=1}^{n} \boldsymbol{V}_i\right), \qquad n \geq 2. \end{aligned} \tag{41}$$

Equating the spaces $\{\boldsymbol{V}_i, i = 1, 2, \cdots, n\}$ to $\{\text{span}(\boldsymbol{B}_i), i = 1, 2, \cdots, n\}$ and using the above outlined steps we obtain the required rank result for $n = M$. From the rank relation, we see that the sum of pairwise gcd's is the number of linearly dependent vectors in the union of the spans of blocks of the separation matrix $\boldsymbol{S}_M$ taken a pair at a time. We can also see that the quantity $Q$ in the underbraces is the number of linearly dependent column vectors in the separation matrix $\boldsymbol{S}_M$ that have been counted multiple times in the sum containing the pairwise gcd's. This quantity $Q$ therefore has to be a positive quantity and, hence, the lower bound in (21) follows.

---

$$r(\boldsymbol{S}_M) = \sum_{i=1}^{M} N_i - \sum_{i,j,i<j} \gcd(N_i, N_j) + \underbrace{\sum_{i,j,k,i<j<k} \gcd(N_i, N_j, N_k) + \cdots (-1)^{M-1} \gcd(N_1, \cdots N_M)}_{Q} \tag{33a}$$

In the case where the component periods are pairwise co-prime, all the gcd's are 1 and using the binomial expansion for $(1-1)^M$, we obtain the result from the previous theorem

$$r(\boldsymbol{S}_M) = \sum_{i=1}^{M} N_i - \sum_{i=2}^{M} (-1)^i \binom{M}{i} = \sum_{i=1}^{M} N_i - (M-1). \tag{42}$$

## REFERENCES


[1] L. Cohen, "What is a multicomponent signal," in *Proc. ICASSP*, vol. 5, Mar. 1992, pp. 113–116.

[2] L. Cohen and C. Lee, "Instantaneous frequency, its standard deviation and multicomponent signals," in *Proc. SPIE*, vol. 975, 1988, pp. 186–208.

[3] A. de Cheveigne, "Separation of concurrent harmonic sounds: Fundamental frequency estimation and a time-domain cancellation model of auditory processing," *J. Acoust. Soc. Amer.*, vol. 93, pp. 3271–3290, June 1993.

[4] A. C. Bovik, N. Gopal, T. Emmoth, and A. Restrepo, "Localized measurement of emergent image frequencies by Gabor wavelets," *IEEE Trans. Inform. Theory*, vol. 38, pp. 698–712, 1992.

[5] A. C. Bovik, P. Maragos, and T. F. Quatieri, "AM–FM energy detection and separation in noise using multiband energy operator," *IEEE Trans. Signal Processing*, vol. 41, pp. 3245–3265, Dec. 1993.

[6] P. Maragos, J. F. Kaiser, and T. F. Quatieri, "On amplitude and frequency demodulation using energy operators," *IEEE Trans. Signal Processing*, vol. 41, pp. 1532–1550, Apr. 1993.

[7] P. Maragos, J. F. Kaiser, and T. F. Quatieri, "Energy separations in signal modulations with application to speech analysis," *IEEE Trans. Signal Processing*, vol. 41, pp. 3024–3051, Oct. 1993.

[8] H. B. Lee, "Eigenvalues and eigenvectors of covariance matrices for signals closely spaced in frequency," *IEEE Trans. Signal Processing*, vol. 40, pp. 2518–2535, Oct. 1992.

[9] J. P. Havlicek, D. S. Harding, and A. C. Bovik, "Extracting essential modulated structure," in *Proc. IEEE 30th Asilomar Conf. Signals, Syst., Comput.*, 1996.

[10] B. Widrow and S. D. Stearns, *Adaptive Signal Processing*. Englewood Cliffs, NJ: Prentice-Hall, 1985.

[11] B. Santhanam and P. Maragos, "Energy demodulation of two-component AM–FM signal mixtures," *IEEE Signal Processing Lett.*, vol. 3, pp. 294–298, Nov. 1996.

[12] M.-Y. Zou, C. Zhenming, and R. Unbehauen, "Separation of periodic signals by using an algebraic method," in *Proc. ISCAS*, vol. 5, 1991, pp. 2427–2430.

[13] A. Potamianos and P. Maragos, "Speech formant frequency and bandwidth tracking using multiband energy demodulation," *J. Acoust. Soc. Amer.*, vol. 99, pp. 3795–3806, June 1996.

[14] A. V. Oppenheim and R. W. Schafer, *Discrete-Time Signal Processing*. Englewood Cliffs, NJ: Prentice-Hall, 1989.

[15] M.-Y. Zou and R. Unbehauen, "An algebraic theory for separation of periodic signals," *Archiv fur Elektronik und Ubertragungstechnik*, vol. 45, no. 6, pp. 351–358, Nov./Dec. 1996.

[16] S. Lu and P. C. Doerschuk, "Nonlinear modeling and processing of speech based on sums of AM–FM formant models," *IEEE Trans. Signal Processing*, vol. 44, pp. 773–782, Apr. 1996.

[17] S. Lu and P. C. Doerschuk, "Modeling and processing speech with sums of AM–FM formant models," in *Proc. ICASSP*, May 1995, pp. 764–767.

[18] P. Maragos and A. Bovik, "Image demodulation using multidimensional energy separation," *J. Opt. Soc. Amer.*, vol. 12, pp. 1867–1876, Sept. 1995.

[19] J. N. Bradley and R. L. Kirlin, "Phase-locked loop cancellation of interfering tones," *IEEE Trans. Signal Processing*, vol. 41, pp. 391–394, Jan. 1993.

[20] J. N. Bradley, "Suppression of adjacent-channel and cochannel interference via extended Kalman filtering," in *Proc. ICASSP*, vol. 4, 1992, pp. 693–696.

[21] B. A. Hedstrom and R. L. Kirlin, "Performance measures for coupled digital phase-locked loops for the separation of co-channel signals," in *Advanced Algorithms and Architectures for Signal Processing*, 1992, pp. 188–197.

[22] B. A. Hedstrom and R. L. Kirlin, "Detection, enumeration and estimation of multiple co-channel signals," in *Proc. 6th Signal Processing Workshop Statistical Signal and Array Processing*, Oct. 1992.

[23] B. A. Hedstrom and R. L. Kirlin, "Co-channel signal separation using cross-coupled digital phase-locked loops," *IEEE Trans. Commun.*, vol. 44, pp. 1373–1384, Oct. 1996.

[24] Y. Bar-ness, F. A. Cassara, H. Schachter, and R. Difazio, "Cross-coupled phase-locked loop with closed loop amplitude control," *IEEE Trans. Commun.*, vol. COM-32, pp. 195–198, Feb. 1982.

[25] S. C. Gupta, "Phase-locked loops," *Proc. IEEE*, vol. 63, pp. 291–306, Feb. 1975.

[26] W. C. Lindsey and C. M. Chie, "A survey of digital phase-locked loops," *Proc. IEEE*, pp. 410–431, Apr. 1981.

[27] F. M. Gardner, *Phaselock Techniques*, 2nd ed. New York: Wiley, 1979.

[28] M. W. Y. Poon, R. H. Khan, and S. Le-Ngoc, "A SVD based method for supressing ocean clutter in high frequency radar," *IEEE Trans. Signal Processing*, vol. 41, pp. 1421–1425, Mar. 1993.

[29] M. H. Hayes, *Statistical Digital Signal Processing and Modeling*. New York: Wiley, 1996.

[30] S. Haykin, *Adaptive Filter Theory*. Englewood Cliffs, NJ: Prentice-Hall, 1991.

[31] I. N. Herstein, *Topics in Algebra*, 2nd ed. New York: Wiley, 1975.

[32] C. L. Dimonte and K. S. Arun, "Tracking the frequencies of superimposed time-varying harmonics," in *Proc. ICASSP*, vol. 2, 1990, pp. 2539–2542.

[33] B. Friedlander and J. M. Francos, "Estimation of amplitude and phase parameters of multicomponent signals," *IEEE Trans. Signal Processing*, vol. 43, pp. 917–926, June 1995.

[34] R. Kumaresan, A. G. Sadasiv, C. S. Ramalingam, and J. F. Kaiser, "Instantaneous nonlinear operators for tracking multicomponent signal parameters," in *Proc. 6th SP Workshop on Statistical Signal and Array Processing*, Oct. 1992, pp. 404–407.

[35] R. M. Liang and K. S. Arun, "Parameter estimation for superimposed chirp signals," in *Proc. ICASSP*, Mar. 1992, pp. 273–276.

[36] H. W. Hawkes, "Study of adjacent and co-channel FM interference," *Proc. Inst. Elect. Eng.*, vol. 138, no. 4, pp. 319–326, Aug. 1991.

[37] T. S. Sundresh, F. A. Cassara, and H. Schachter, "Maximum *a posteriori* estimator for suppression of interchannel interference in FM receiver," *IEEE Trans. Commun.*, vol. COM-25, pp. 1480–1485, Dec. 1977.

[38] A. Potamianos and P. Maragos, "A comparison of the energy operator and Hilbert transform approaches for signal and speech demodulation," *Signal Processing*, vol. 37, pp. 95–120, May 1994.

[39] A. Zayezdny and I. Druckmann, "A new method of signal description and its applications to signal processing," *Signal Processing*, vol. 22, pp. 153–178, 1991.

[40] S. Haykin, *Communication Systems*, 2nd ed. New York: Wiley, 1983.



**Balu Santhanam** (S'92–M'98) was born in Chrompet, India in 1971. He received the B.S. degree in electrical engineering from St. Louis University, St. Louis, MO, in 1992. He obtained the M.S. and Ph.D. degrees in electrical engineering from the Georgia Institute of Technology, Atlanta, in 1994 and 1998, respectively, where he was a Research Assistant with the DSP Laboratory.

From 1998 to 1999, he was a Lecturer and Postdoctoral Researcher with the Department of Electrical and Computer Engineering at the University of California, Davis. In the Fall of 1999, he joined the faculty of the Department of Electrical and Computer Engineering at the University of New Mexico, Albuquerque, where he is presently an Assistant Professor. His current research interests include general signal processing, statistical DSP, communication systems, multicomponent AM–FM signal separation, modulation/demodulation, and time–frequency analysis.

**Petros Maragos** (S'81–M'85–SM'91–F'95) received the Diploma degree in electrical engineering from the National Technical University of Athens, Athens, Greece, in 1980, and the M.S. and Ph.D. degrees in electrical engineering from the Georgia Institute of Technology, Atlanta, in 1982 and 1985,l respectively.

In 1985, he joined the faculty of the Division of Applied Sciences at Harvard University, Cambridge, MA, where he worked for eight years as a Professor of Electrical Engineering, affiliated with the interdisciplinary Harvard Robotics Laboratory. He has also been a Consultant to several industry research groups including Xerox's research on document image analysis. From 1993 to 1998, he was on the faculty at the Georgia Institute of Technology working as a Professor of Electrical Engineering. During parts of 1996–1998, he also worked as a Senior Researcher at the Institute for Language and Speech Processing in Athens. In 1998, he joined the faculty of the National Technical University of Athens where he is a Professor of electrical and computer engineering. His current research and teaching interests include the general areas of signal processing, systems theory, communications, control, pattern recognition, and their applications to image processing and computer vision, and computer speech processing and recognition.

Dr. Maragos has served as Associate Editor for the IEEE TRANSACTIONS ON SIGNAL PROCESSING, as Editorial Board Member for the *Journal on Visual Communications and Image Representation*, and as Guest Editor for the IEEE TRANSACTIONS ON IMAGE PROCESSING. He has also served as General Chairman for the 1992 SPIE Conference on Visual Communications and Image Processing, and Cochairman for the 1996 International Symposium on Mathematical Morphology. He is a member of two IEEE DSP Committees and President of the International Society for Mathematical Morphology. Dr. Maragos' research work has received several awards, including: a 1987 U.S. National Science Foundation Presidential Young Investigator Award, the 1988 IEEE Signal Processing Society's Young Author's Best Paper Award for the paper, "Morphological Filters;" the 1994 IEEE Signal Processing Society's Best Paper Award and the 1995 IEEE Baker Award, both for the paper, "Energy separation in signal modulations with application to speech analysis" (co-recipient), and the 1996 Pattern Recognition Society's Honorable Mention Award for the paper "Min–Max classifiers" (co-recipient).